Structure and binding of two-dimensional Lennard-Jones clusters

Joyce C. Yang

Yang Academy, 111 Central Avenue, Gaithersburg, Maryland 20877, USA

April 1, 2012

Abstract

We have developed a growth sequence that predicts the initial configuration of a local minimum energy structure for a two-dimensional Lennard-Jones cluster of n particles. We compared the local minimum energies of clusters of size 4-20 and used the minimum energy structures as the basis of this growth sequence. In this sequence, we append a particle to the previous size's initial structure to determine the current size's structure. We use the "greedy" method in which the choice with the greatest immediate advantage determines the position of a new particle. Particles in our growth sequence lie in concentric regular hexagonal shells, forming the maximum number of nearest-neighbor bonds. Through this sequence, we have reached energy values lower than or equal to all other published values in two dimensions. We have obtained lower energies than our growth sequence energy for certain sizes by modifying the initial structures determined by the growth sequence.

1. Introduction

We consider n-particle systems that interact via the Lennard-Jones potential,

$$V_{ij} = r_{ij}^{-12} - 2r_{ij}^{-6} \qquad (1)$$

where V_{ij} is the potential in units of the depth of the potential well and

$$r_{ij} = \left| \boldsymbol{r}_i - \boldsymbol{r}_j \right| \qquad (2)$$

is the distance between particles i and j in units of the equilibrium distance. We seek the global minimum of the sum of V_{ij} over all pairs of particles in a two-dimensional cluster. Ref. [1] shows that the problem of determining the ground state of a cluster is NP-hard. The solution of this problem would reveal insights to optimization methods in other problems, particularly elusive of which is protein folding [2].

The Lennard-Jones potential is used to describe rare-gas clusters and to approximate the interactions in colloid and metal clusters. Refs. [3, 4] present images of colloids that lie on a hexagonal lattice, resembling Lennard-Jones clusters. Refs. [5, 6], among many other works, thoroughly examine the structures of three-dimensional Lennard-Jones clusters. We present a simple greedy, or "SG" growth sequence that predicts the initial configuration of a local minimum energy structure for a two-dimensional cluster. Several attempts to devise an algorithm for the ground state of a two-dimensional cluster exist. Ref. [7] uses a chain folding model, which we denote by "CF". In this model, consecutive particles always bond as nearest neighbors, forming a chain. We performed the same minimization used for our structures on the structures depicted in Ref. [7], assuming nearest-neighbor distances of 1. Our growth sequence

produces energies lower than or equal to all those resulting from CF. Ref. [8] presents a genetic algorithm, or "GA," predicting an initial structure for a global minimum, followed by a local minimization. Our growth sequence produces energies lower than or equal to all values presented by Ref. [8]. Refs. [9, 10] present an approximate minimization using a concentric rings model, which we denote by "CR", and the resulting energies. In this method, particles remain on concentric circular rings; initial polar coordinates of particles on the ith ring are given by

$$r = ia \qquad (3)$$

and

$$\theta = \frac{\pi\alpha}{3i} \qquad (4)$$

where a is the radial distance between consecutive rings and the approximate distance between all nearest neighbors, and

$$\alpha = 1,2,...6i-1 \qquad (5)$$

Varying a leads to expansion or contraction of the rings and different resulting energies. Our growth sequence produces energies lower than or equal to all those resulting from CR.

2. Method

2.1 Local minimization

We wrote a local minimization computer program that determines the motion of particle $\boldsymbol{i}$ according to

$$\Delta x_i = \frac{\frac{1}{2} F_{ix} (\Delta t)^2}{m} \qquad (6)$$

$$\Delta y_i = \frac{\frac{1}{2} F_{iy} (\Delta t)^2}{m} \qquad (7)$$

where x_i and y_i are the $x-$ and $y-$ components of i's position; F_{ix} and F_{iy} are the $x-$ and $y-$ components of the force on i; m, the mass of i, is set to 1 for all particles; and Δt, the time step, is set to 0.05. The force on i from every other particle j is given by

$$\boldsymbol{F}_{ij} = -\nabla_i V_{ij} \qquad (8)$$

Our method is similar to the steepest-descent method described by Ref. [11].

We initialized the coordinates of a cluster and set upper bounds on the number of steps and the maximum force on all particles. When the maximum force on all particles reaches the bound of 10^{-7}, the resulting energy lies at a local minimum. The first small clusters require fewer than 800 steps; the largest cluster in the present work requires more than 22,000 steps.

2.2 Comparison of small clusters

Clusters of sizes 2 and 3 have clear minimum energies: a cluster of two particles has a minimum energy equal to the depth of the potential well, and a cluster of three

particles attains its minimum energy when each of the three pairs of particles in the cluster attains its minimum energy; that is, when the three particles form an equilateral triangle. The corresponding energy values are -1 and -3.

We compared cluster structures of sizes 4-20, shown in Fig.1. Setting initial nearest-neighbor distances all equal to 1, we entered the coordinates of the structures into our minimization program and compared the resulting energies. We used hexagonal coordinates for the structures starting from size 6 after confirming that assigning particles on a hexagonal lattice, which allows six nearest neighbors to a point, in contrast to a square lattice, which allows four, led to minimum energies for sizes 4 and 5. We converted the hexagonal coordinates to rectangular coordinates using

$$(x_{rect}, y_{rect}) = (x_{hex} + \frac{y_{hex}}{2}, \frac{\sqrt{3} y_{hex}}{2}) \qquad (9),$$

the derivation of which is straightforward.

The resulting energies support the following conclusions about the conditions for stability: symmetry indicates stability to a certain degree, because the long-range attraction from two sides of a certain region will cause a central position to be favorable. However, the most important factor when considering a position for a new particle is the contribution of each pair potential: nearest neighbors have a pair potential approximately -1, at the bottom of the potential well, while long-range binding energy decreases rapidly.

2.3 Growth sequence

The minimum energy structures of the sizes 1-20 were sufficient to construct a growth sequence. The growth sequence determines that a cluster of a certain size must be the cluster of the previous size with one particle appended. We use the "greedy" method, considering only the positions at which a particle would contribute the most binding energy. In addition, we append particles to the initial, not the minimized, structure, as our structures vary little before and after minimization. Hence, our greedy method is "simple." We attempted to append particles to each structure to produce a structure that, upon rotation or reflection, would replicate the next size's minimum energy structure and that would follow established patterns when possible. A special case, size 12's minimum energy structure did not contain the minimum energy structure for size 11. Keeping the minimum energy structure for size 10 and removing one other particle from size 12's structure, we found a new structure of size 11. The new structure is shown in Fig. 2, consisting of the sites 1-11. The previous structure, shown as 11a in Fig. 1b, resembles the structure consisting of sites 1- 10 and 13 in Fig. 2. Sites 11 and 13 have equal interactions with the hexagon formed by sites 1-7, but site 11 is closer to each of sites 8, 9, and 10. Thus, site 11 is more favorable than site 13 and the new structure is the minimum energy structure. This new structure did, indeed, have the lowest energy when compared with structures of the same size. We include the new structure in our growth sequence. For the remainder of the sizes up to 20, our minimum energy structures describe a growth sequence. We expanded this growth sequence to describe a cluster of size n. (See J.C. Yang, "Two-Dimensional Lennard-Jones Clusters," for analytical formulas for generating the growth sequence.) Fig. 2 contains

the structures for $1 \leq n \leq 127$; the structure for size n contains the circles labeled 1 to n in the diagram.

The growth sequence is defined as follows: with the first particle at the origin of a hexagonal coordinate system, the second through seventh particles take consecutive positions neighboring the first particle. The eighth particle attaches to one side of the established hexagon. We proceed counterclockwise. The ninth particle attaches to the next side. Binding with regard to maximization of nearest-neighbor bonds results in a new, identically oriented hexagonal shell around the original core. We now define the construction of a shell: A "site" is a point neighboring two particles of the previous shell, and "central" is used with respect to the regular hexagonal formation already fixed. The first side of the hexagon begins in the first quadrant and at the center site. If two sites are central, we choose that nearer to the positive x-axis. The next particle occupies the site equally as central as the previous particle or the most central site adjacent to the previous particle toward the previous side. The effect is alternating between left and right ends of a side. For side 1, the oscillation stops before a particle reaches the positive x-axis. Side 1 of every shell forms an equilateral triangle with the positive x- and y-axes. Side 2 lies on a horizontal line in the second quadrant, and among the sites on side 2, we choose the seed particle to be the center site or that center site nearer to the previous side. Again, we alternate between the left and right ends of the side. The last particle takes the position at the corner where sides 1 and 2 meet. Sides 3-5 have the same construction as side 2, with their last particle on the corner with the previous side. Side 3 forms a rhombus with side 2 and the negative x- and positive y- axes. Side 4 forms an equilateral triangle with the negative x- and negative y-axes. Side 5

lies on a horizontal line in the fourth quadrant. Side 6 forms a rhombus with side 5 and the positive x- and negative y- axes. The construction of side 6 follows the same pattern as side 2, and in addition places the last particle on the corner with side 1, on the x-axis. Thus, all shells end on the x-axis.

3. Results

The difference between the energy we calculated for a CF structure from Ref. [7] and the energy of our SG structure is shown for sizes 3-25 in Fig. 3, and for sizes 25-92 in Fig. 4. Like the SG growth sequence, CF appends a particle to a structure to determine the next size's structure. However, the greedy method marks our growth sequence while particles in the CF from Ref. [7] assume a clockwise spiral equivalent to tracing a shell in our SG growth sequence, then crossing into the next shell. For the circles numbered 1-25, for example, the path in terms of the sites in Fig. 2 is 1, 6, 5, 4, 3, 2, 7, 17, 18, 15, 16, 13, 14, 11, 12, 9, 10, 8, 19, 35, 34, 36, 32, 31, 33. Fig. 3a shows pronounced peaks in energy for sizes 9, 17, 22, and 25, and lesser peaks for sizes 15 and 23. We verify that each of the SG structures for sizes 9 and 15 has lower energy than the corresponding CF structure, and similar arguments will apply to 17, 22, 23, 25, and those sizes up to 92 for which we found lower energies. Checking the structure for 9 reveals that the CF structure resembles the structure consisting of sites 1-8 and 10 in Fig. 2. Sites 9 and 10 have equal interactions with the triangle described by sites 1-3 and 6-8, but site 9 is closer to each of sites 4 and 5. Thus, the SG structure, consisting of sites 1-9, has lower energy than the CF structure. The CF structure of size 15 resembles the structure consisting of sites 1-14 and 16. Sites 15 and 16 have equal

interactions with the sites 1-7, 9, and 11-14, but site 15 is closer to each of sites 8 and 10. Thus, the SG structure, consisting of sites 1- 15, has lower energy than the CF structure.

Fig. 3 shows the difference between the energy given by the GA from Ref. [8] and the energy of our SG structure for sizes 3-25. The structures predicted by the GA are depicted in Ref. [8]. From Fig. 3b, it is clear that sizes 18, 20, 22, and 25 correspond to small peaks in energy and that sizes 19 and 21 correspond to two large peaks in energy. The reason for the first large peak is not clear as Ref. [8] obtains the same structure as the SG structure, and further indicates that 19 is a “magic number” for which the structure is especially stable. We verify the result for size 21. The GA structure of size 21 resembles the structure consisting of sites 1-19, 20, and 22 in Fig. 2. Site 22 contributes two nearest-neighbor bonds to the structure, while site 21 contributes two with the existing hexagonal core and one more with site 20. Thus, the SG structure, consisting of sites 1-21, has energy lower than the GA structure by about 1 unit, the contribution of one nearest-neighbor potential.

We calculated the total energy for the cluster sizes given by Ref. [9], equal to the average energy per particle times the cluster size. Table 1 shows the difference between this energy value and the energy of our SG structure for sizes from 7 to 2269 corresponding to complete rings in CR, or completed shells in our SG growth sequence.

Refs. [9, 10] also predict an asymptotic value for the energy per particle for a large cluster determined by CR, based on cluster sizes up to 55,000. We calculated the energy per particle for our SG structures and found that the energy per particle even for size 91, for example, was lower than this asymptotic value. The initial energy value for

the SG structure for size 91 with a nearest-neighbor distance of 1 is -2.91190, while the asymptotic value for CR structures is -2.85726.

We present the lowest energies we found in Table 2. We modified certain SG structures by moving particles to the sites that would be occupied next. For size 34, for example, we moved the particle at site 33 to site 35; for size 57 we moved the particles at sites 52 and 56 to sites 58 and 59; for size 86 we moved the particles at sites 75, 80, and 85 to sites 87, 88, and 89; and for size 121 we moved the particles at sites 102, 108, 114, and 120 to sites 122, 123, 124, and 125.

4. Discussion

We have reached energy values lower than or equal to all other published values in two dimensions. Our growth sequence allows flexibility while particles take consecutive positions in CF. We focus on forming the most nearest-neighbor bonds, thus reaching a lower energy for size 21 than the GA does. We allow clusters to relax during minimization, while structures remain rigid in CR. Our growth sequence serves as a basis for improvement. By modifying our initial growth sequence structures, we have reached lower energies. We intend to continue moving particles from the growth sequence structures.

5. Conclusion

We have used a simple greedy growth sequence in reaching our values. The intuitive property of the growth sequence simplifies many procedures. Little effort can

produce a formula dictating the coordinates of a cluster of any size, and modifying a particle's position requires only changing one set of coordinates.

We have developed a growth sequence that predicts a local minimum energy for a cluster of n particles in two dimensions. We moved individual particles to form new initial structures and obtained lower energies for certain sizes starting from 34. We will continue to use our growth sequence in our search for global minima.

References

[1] L. T. Wille and J. Vennik, “Computational complexity of the ground-state determination of atomic clusters,” Journal of Physics A: Mathematical and General, vol. 18, pp. 419-422, 1985.

[2] Y. Zhou and M. Karplus, “Interpreting the folding kinetics of helical proteins,” Nature, vol. 401, pp. 400-403, 1999.

[3] G. Ononda, “Direct observation of two-dimensional, dynamical clustering and ordering with colloids,” Physical Review Letters, vol. 55, pp. 226-229, 1985.

[4] G. Meng, N. Arkus, M. P. Brenner, and V.N. Manoharan, “The free-energy landscape of clusters of attractive hard spheres,” Science, vol. 327, pp. 560-563, 2010.

[5] D. J. Wales and J. P. K. Doye, “Global optimization by basin-hopping and the lowest energy structures of Lennard-Jones clusters containing up to 110 atoms,” Journal of Physical Chemistry A, vol. 101, pp. 5111-5116, 1997.

[6] J. A. Northby, “Structure and binding of Lennard-Jones clusters,” Journal of Chemical Physics, vol. 87, pp. 6166-6177, 1987.

[7] C. Amano, T. Urushibara, T. Shiobara, R. Hatano, Y. Watanabe, and O. Miyauchi, “Closed-shell numbers and two-dimensional rare gas microclusters,” Journal of Colloid and Interface Science, vol. 258, pp. 50-55, 2003.

[8] M. Iwamatsu, “Structural optimization of model colloidal clusters at the air-water interface using genetic algorithms,” Journal of Colloid and Interface Science, vol. 260, pp. 305-311, 2003.

[9] Y. Deng and C. Rivera, “Approximate energy minimization for large Lennard-Jones clusters,” Journal of Global Optimization, vol. 16, pp. 325-341, 2000.

[10] Y. Deng and C. Rivera, “Simple energy minimization for huge Lennard-Jones clusters by dramatic parameter reduction,”Applied Mathematics Letters, vol. 12, pp. 119-124, 1999.

[11] F. H. Stillinger and T. A. Weber, “Hidden structure in liquids,” Physical Review A, vol. 25, pp. 978-989, 1982.

.

Figure and table captions

Fig. 1 Structures initially considered in our search for the minimum energy structure for each cluster size; the structure with the lowest energy among those shown for each size is marked by a dagger (†).

Fig. 1a Sizes 4-8

Fig. 1b Sizes 9-12

‡We later found that this structure has a higher energy than that of another structure, which is shown in Fig. 2.

Fig. 1c Sizes 13-16

Fig. 1d Sizes 17-20

Fig. 2 Simple greedy growth sequence for $1 \leq n \leq 127$, where n is the cluster size. The growth sequence structure for size n contains the circles labeled 1 to n in the diagram. Hexagonal shells are alternately shaded dark and light. (See J.C. Yang, "Two-Dimensional Lennard-Jones Clusters," for analytical formulas for generating the growth sequence.)

Fig. 3 Solid diamonds represent energy difference $\Delta E = E_{CF} - E_{SG}$; open circles represent energy difference $\Delta E = E_{GA} - E_{SG}$. E_{CF} is the energy we calculated for a structure given by the chain folding method used in Ref. [7], E_{SG} is the energy of a

structure given by our simple greedy method, and E_{GA} is the energy of a structure given by the genetic algorithm used in Ref. [8]. The cluster size is represented by n.

Fig. 3a Detailed view

Fig. 3b Overall view

Fig. 4 Energy difference $\Delta E = E_{CF} - E_{SG}$, where E_{CF} is the energy we calculated for a structure given by the chain folding method used in Ref. [7] and E_{SG} is the energy of a structure given by our simple greedy method. $25 \leq n \leq 92$, where n is the cluster size.

Table 1. Energy E_{SG} of a structure given by the simple greedy method and energy E_{CR} of a structure given by the concentric rings method described in Refs. [9]. E_{CR} is based on the value of the energy per particle given by Ref. [9]. Sizes correspond to completed shells. $7 \leq n \leq 2269$, where n is the cluster size.

Table 2. $E_{min,}$ the lowest energy found for $4 \leq n \leq 127$, where n is the cluster size; lowest energy structures were determined using the simple greedy with modification method for the sizes marked with an asterisk (*); structures for other sizes were determined using the simple greedy method.

Table 1

n	E_{SG}	E_{CR}
7	-12.53487	-12.53487
19	-45.35112	-38.93799
37	-98.48347	-83.37058
61	-171.91566	-145.35281
91	-265.64329	-224.69401
127	-379.66486	-321.30797
169	-513.97981	-435.15016
217	-668.58784	-566.19553
271	-843.48883	-714.42917
331	-1038.68270	-879.84169
397	-1254.16939	-1062.42718
469	-1489.94889	-1262.18030
547	-1746.02117	-1479.09894
631	-2022.38622	-1713.18077
721	-2319.04404	-1964.42290
817	-2635.99461	-2232.82505
919	-2973.23794	-2518.38625
1027	-3330.77402	-
1141	-3708.60285	-3140.98131
1261	-4106.72443	-3478.01328
1387	-4525.13875	-3832.20194
1519	-4963.84581	-4203.54693
1657	-5422.84562	-4592.04576
1801	-5902.13818	-4997.70116
1951	-6401.72347	-5420.51012
2107	-6921.60151	-5860.47512
2269	-7461.77229	-6317.59485

Table 2

n	E_{min}	n	E_{min}	n	E_{min}	n	E_{min}
4	-5.07342	35	-91.91908	66*	-186.63522	97*	-283.83961
5	-7.17802	36	-95.20043	67*	-189.92075	98*	-287.12566
6	-9.35827	37	-98.48347	68*	-193.20622	99*	-290.41164
7	-12.53487	38	-100.81202	69	-196.49130	100*	-293.69744
8	-14.68399	39	-104.06284	70	-199.77630	101	-296.98297
9	-16.90932	40	-107.34252	71*	-202.25584	102	-300.26846
10	-20.10161	41*	-109.73153	72*	-205.54149	103*	-302.84308
11	-22.33654	42	-113.01376	73*	-208.82696	104*	-306.12913
12	-25.56670	43	-116.29606	74	-212.11227	105*	-309.41513
13	-27.80407	44	-119.57928	75	-215.39749	106*	-312.70084
14	-31.03645	45*	-121.96715	76*	-217.87721	107	-315.98646
15	-33.27783	46	-125.25132	77*	-221.16275	108	-319.27202
16	-36.51169	47	-128.53375	78*	-224.44826	109*	-321.84663
17	-38.83421	48	-131.81778	79	-227.73356	110*	-325.13268
18	-42.07808	49*	-134.20573	80	-231.01880	111*	-328.41867
19	-45.35112	50	-137.48998	81*	-233.49855	112*	-331.70446
20	-47.59505	51	-140.77247	82*	-236.78422	113	-334.99007
21	-50.83360	52	-144.05656	83*	-240.06981	114	-338.27564
22	-53.15874	53*	-146.44477	84	-243.35511	115*	-340.85037
23	-56.40738	54	-149.72905	85	-246.64036	116*	-344.13641
24	-59.68155	55	-153.01177	86*	-249.21458	117*	-347.42240
25	-62.00856	56	-156.29590	87*	-252.50062	118*	-350.70820
26	-65.25791	57*	-158.77513	88*	-255.78660	119	-353.99381
27	-68.53625	58*	-162.06038	89*	-259.07227	120	-357.27939
28	-70.86361	59*	-165.34563	90	-262.35781	121*	-359.94960
29	-74.11324	60	-168.63071	91	-265.64329	122*	-363.23569
30	-77.39182	61	-171.91566	92*	-268.12290	123*	-366.52175
31	-79.71969	62*	-174.30344	93*	-271.40871	124*	-369.80775
32	-82.97014	63	-177.58854	94*	-274.69431	125*	-373.09352
33	-86.24891	64	-180.87136	95	-277.97984	126	-376.37921
34*	-88.63780	65	-184.15574	96	-281.26518	127	-379.66486

*energy for this size was reached through the simple greedy method with modification

Figure 1

(a)

4a 4b†

5a 5b† 5c

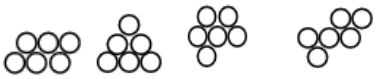

6a 6b 6c† 6d

7a† 7b 7c 7d

8a† 8b 8c 8d 8e

Figure 1

(b)

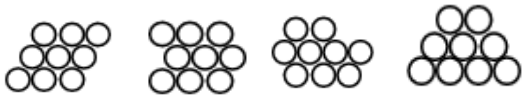

9a 9b† 9c 9d

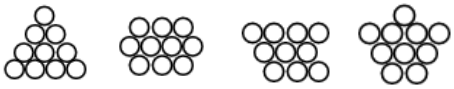

10a 10b† 10c 10d

11a†‡ 11b

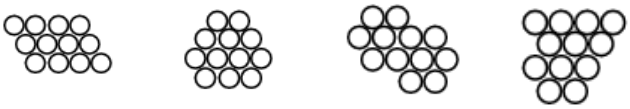

12a 12b† 12c 12d

Figure 1

(c)

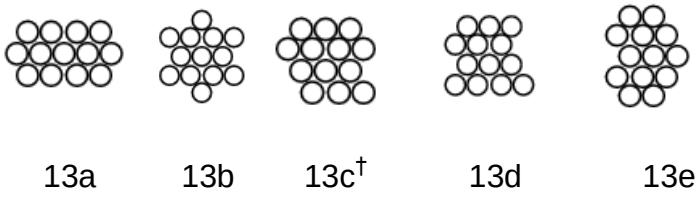

13a 13b 13c† 13d 13e

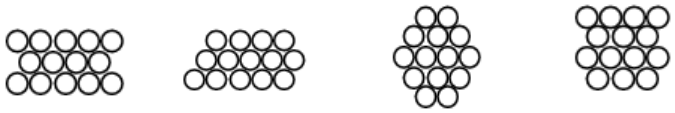

14a 14b 14c† 14d

15a 15b 15c 15d 15e 15f† 15g

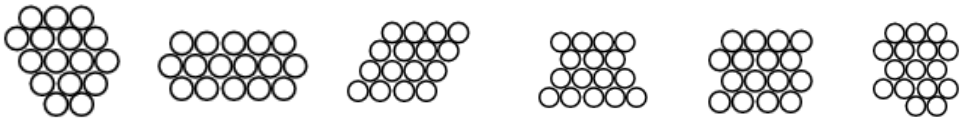

16a† 16b 16c 16d 16e 16f

Figure 1

(d)

17a† 17b 17c

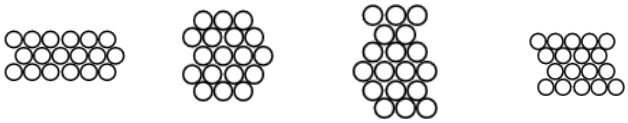

18a 18b† 18c 18d

19a 19b† 19c

20a† 20b 20c 20d 20e

Figure 2

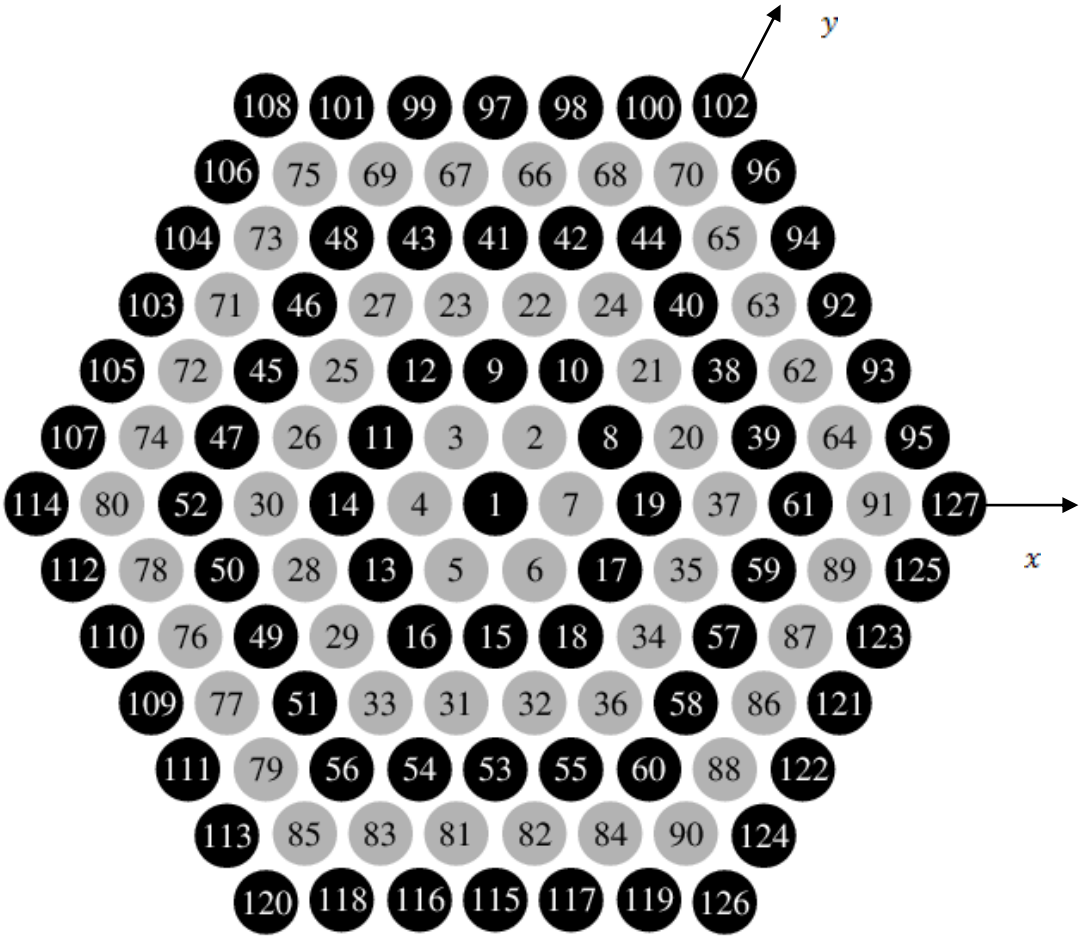
y
x
108 101 99 97 98 100 102
106 75 69 67 66 68 70 96
104 73 48 43 41 42 44 65 94
103 71 46 27 23 22 24 40 63 92
105 72 45 25 12 9 10 21 38 62 93
107 74 47 26 11 3 2 8 20 39 64 95
114 80 52 30 14 4 1 7 19 37 61 91 127
112 78 50 28 13 5 6 17 35 59 89 125
110 76 49 29 16 15 18 34 57 87 123
109 77 51 33 31 32 36 58 86 121
111 79 56 54 53 55 60 88 122
113 85 83 81 82 84 90 124
120 118 116 115 117 119 126

Figure 3

(a)

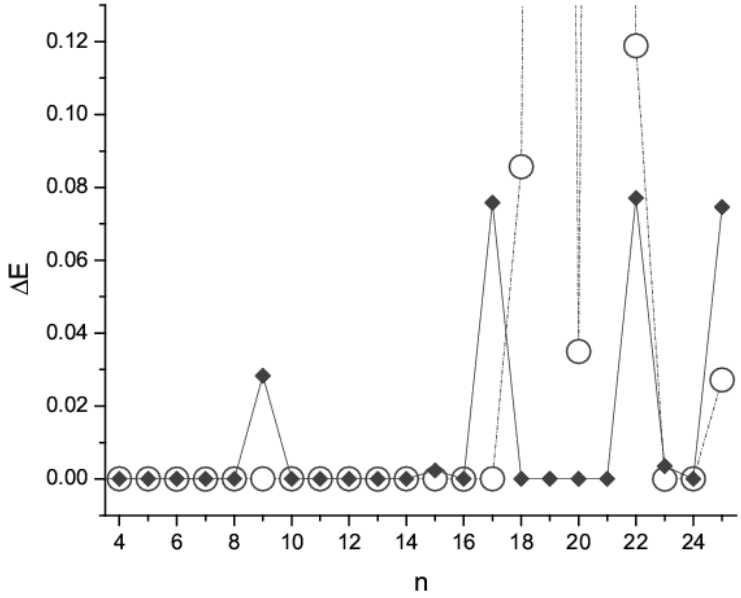

Figure 3

(b)

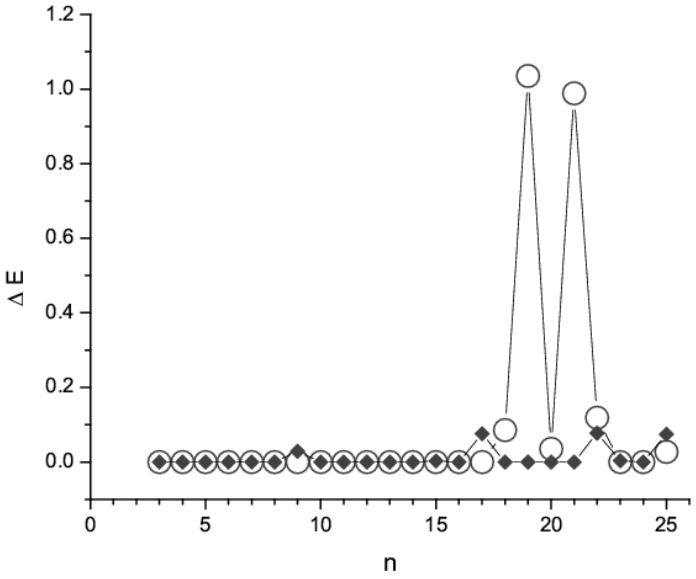

Figure 4